Bistatic Doppler Estimation Based on Extremely Large Aperture Arrays

Caterina Giovannetti*†‡, Tommaso Bacchielli†‡, Nicolò Decarli*‡, Andrea Giorgetti†‡, Davide Dardari†‡

* IEIIT, National Research Council (CNR), 40136 Bologna, Italy
† DEI, Università di Bologna, 40136 Bologna, Italy
‡ National Laboratory of Wireless Communications (WiLab), CNIT, 40136 Bologna, Italy

***Abstract*—Future networks are expected to leverage joint communication and sensing (JCS) enabled by advances such as extremely large aperture arrays (ELAAs) and high-frequency operations. These technologies introduce significant near-field propagation effects, which can be exploited to enhance sensing performance. This paper investigates velocity sensing through Doppler analysis in bistatic radar systems. By leveraging ELAAs, we demonstrate how velocity components can be accurately estimated. Performance bounds are derived to quantify the influence of system parameters and bistatic geometries on Doppler-based velocity estimation. The results highlight the advantages of bistatic sensing with ELAAs, offering new insights to drive the design and optimization of JCS for 6G networks.**

I. Introduction

Integration of communication and sensing in a unified framework, referred to as joint communication and sensing (JCS), is emerging as a key innovation in next-generation wireless systems, particularly in the context of sixth generation (6G) and beyond [1]–[3]. JCS enables systems to simultaneously perform communication and sensing tasks, thereby enhancing spectral efficiency and reducing hardware costs while opening new advanced potential applications. Among these, applications requiring precise motion tracking and decision-making, such as autonomous driving, are rapidly gaining interest [4], [5]. For this reason, the ability to accurately estimate the velocity of passive moving objects, which is related to the Doppler shift, represents an important requirement for JCS systems. However, when considering far-field propagation conditions, the estimation of target velocity components is only possible in a multi-static or distributed radar configuration due to the possibility of observing it from multiple directions, at the cost of challenging synchronization issues and expensive hardware. The work in [6] proposes a method for estimating the velocity vector of a moving target using multiple radars in a distributed monostatic radar system, while [7] derives the Cramér-Rao lower bound (CRLB) on target velocity estimation by considering a distributed multiple input multiple output (MIMO) radar with widely dispersed antennas. Moreover, in [8] methods for determining the instantaneous velocity vector of a target using a multi-static radar are presented. On the other hand, in monostatic configurations, the Doppler shift evaluation only enables the estimate of the radial velocity [9]. In [10], instead, authors consider a bistatic radar configuration providing the CRLB for the velocity component along the bistatic bisector, referred as radial velocity as well.

Nevertheless, recent work in [11] demonstrates the possibility of accurately estimating the velocity considering both the radial and transverse velocity components of a moving target in a monostatic configuration exploiting the near-field conditions that arise due to the adoption of extremely large aperture arrays (ELAAs) [12]. In fact, when a large array is adopted, each antenna element allows the Doppler shift to be measured from different perspectives, thus enabling the estimation of the different velocity components. In [13] authors derived analytical performance bounds in terms of CRLB for both velocity components in the single input multiple output (SIMO) monostatic configuration. However, monostatic radar suffers from self-interference and can provide less spatial diversity compared to a bistatic configuration [14]. To the authors' knowledge, there remains a lack of research investigating the theoretical bounds on velocity components estimation using ELAAs in the near field by considering a bistatic radar configuration.

To fill this gap, this paper investigates the fundamental performance limits of velocity estimation in bistatic radar systems employing antenna arrays. Specifically, we demonstrate that by exploiting arrays—particularly ELAAs—in bistatic radar systems, it is possible to estimate not only the radial component of the target velocity, as in single-antenna bistatic radars, but also the transverse component. We show that the estimation accuracy of the transverse velocity improves as the aperture of the array increases at the expense of a slight deterioration of that of the radial component, leading to a more precise determination of the full target velocity. This advancement can significantly enhance the performance of bistatic radar systems in target tracking and motion analysis.

II. System Model

We consider a radar sensing a passive point target moving in a two-dimensional scenario along a generic trajectory, using a SIMO bistatic configuration, namely with a single transmitter and K receiving antennas, possibly composing an ELAA, as

This work was supported by the European Union under the Italian National Recovery and Resilience Plan (NRRP) of NextGenerationEU, partnership on "Telecommunications of the Future" (PE00000001 - program "RESTART"), and by the EU HORIZON-JU-SNS-2022 project TIMES (Grant no. 101096307).

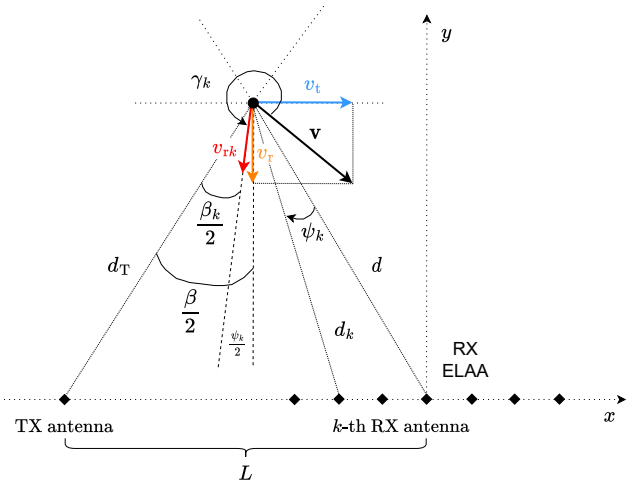

Fig. 1. 2D bistatic scenario, considering a SIMO configuration with a single transmitter and K antenna elements composing the receiving ELAA.

shown in Fig. 1. More specifically, a uniform linear deployment is considered. The antenna spacing is δ and, without loss of generality, let us assume K to be odd. Accordingly, the aperture of the array is defined as $D_\mathrm{a} = (K-1)\delta$. The reference system is placed on the central element of the receiving ELAA, which acts as reference antenna. We denote with $\tilde{\mathbf{p}}_\mathrm{T} = [x_\mathrm{T}, y_\mathrm{T}]^\top$ the position of the single antenna transmitter, while the k-th element of the receiving ELAA is located in $\tilde{\mathbf{p}}_k = [x_k, y_k]^\top$, with $k = -(K-1)/2, \ldots, (K-1)/2$. For instance, if a horizontal array oriented along the x-axis is employed, then $x_k = k\delta$ and $y_k = 0$, $\forall k$. We assume a point target in position $\tilde{\mathbf{p}} = [x, y]^\top$ moving with velocity $\mathbf{v}$. The distance between the transmitter and the target is d_T. The distance between the target and the k-th receiving antenna is d_k; for further convenience, we denote with $d = d_0$ the distance between the target and the reference antenna of the ELAA. The straight line distance between the transmitter and the receiver of length L is called *baseline* of the bistatic radar. The angle β formed between the transmitter, the target, and the receiver (i.e., the angle subtended at the target) is the so-called *bistatic angle* [15]. Finally, the *bistatic bisector* is the angle bisector of the bistatic angle β subtended at the target.

The JCS transmitter sends an orthogonal frequency-division multiplexing (OFDM) signal of power P_T, spanning M symbols and N subcarriers, so that $P = P_\mathrm{T}/N$ is the power allocated at each subcarrier. The symbol time is T_sym and the subcarrier spacing (SCS) is Δf. The signal is modulated at the carrier frequency f_c.

After cyclic prefix removal and FFT processing, the complex low-pass version of the received signal can be written as [16]

$$\begin{aligned} r_{m,n,k} &= y_{m,n,k} + z_{m,n,k} \\ &= \sqrt{P}\alpha_{n,k} u_{m,n} e^{-\mathrm{j}2\pi f_n \tau_k} e^{\mathrm{j}2\pi \nu_{n,k} m T_\mathrm{sym}} + z_{m,n,k} \end{aligned} \tag{1}$$

for $m = 0, 1, \ldots, M-1$ and $n = 0, 1, \ldots, N-1$, where $y_{m,n,k}$ is the useful part of the signal, while $z_{m,n,k} \sim \mathcal{N}\left(0, \sigma^2\right)$ denotes the additive white Gaussian noise (AWGN). In addition, $u_{m,n}$ is the data transmitted in the m-th OFDM symbol and n-th subcarrier, $\alpha_{n,k}$ is the path gain factor experienced at the k-th receiving antenna, considering the n-th subcarrier, $f_n = f_\mathrm{c} + \left(n - \frac{N-1}{2}\right)\Delta f$ is the frequency associated with the n-th subcarrier, and $\tau_k = \frac{d_\mathrm{T}+d_k}{c}$ is the propagation delay at the k-th receiving antenna, where c is the speed of light. The term $\nu_{n,k}$ denotes the Doppler shift at the n-th subcarrier and the k-th receiving antenna. We consider a bandwidth small enough to assume $\frac{f_n - f_\mathrm{c}}{f_\mathrm{c}} \ll 1$ and constant Doppler shift across the subcarriers, thus $\nu_{n,k} \approx \nu_k$, $\forall n$. Considering a practical size of the array and a target located at a distance larger than the array aperture (i.e., $d > D_\mathrm{a}$) in a line-of-sight (LOS) dominated near-field scenario, all antennas experience almost the same path loss, thus we have $\alpha_{n,k} = \alpha\ \forall n, k$. Moreover, considering that the data are known at the receiver and used as pilots, we can assume $u_{m,n} = 1$.

In this bistatic configuration, the k-th Doppler shift ν_k at the k-th receiving antenna is given by [10]

$$\nu_k = \frac{2}{\lambda} v \cos\gamma_k \cos\frac{\beta_k}{2} \tag{2}$$

where $\lambda = c/f_\mathrm{c}$ is the wavelength and $v = ||\mathbf{v}||$ is the magnitude of the velocity tangent to the trajectory in $\tilde{\mathbf{p}}$. It is possible to observe that the Doppler shift in (2) is a function of two key parameters:

- the k-th bistatic angle β_k relative to the k-th antenna, i.e., the angle formed between the transmitter, the target, and the k-th receiver;
- the projection of the velocity along the k-th bistatic bisector $v\cos\gamma_k$, being γ_k the angle between the velocity and the k-th bistatic bisector (see Fig. 1).

Notice that as a large number of receiving antennas K is assumed due to the adoption of an ELAA, the bistatic bisector and the bistatic angle change for each antenna element.

The term $v\cos\gamma_0$ denotes the magnitude of the projection of the velocity along the bistatic bisector of the reference antenna. This is usually referred to as *radial velocity* [10]. We denote such a term with v_r. The component orthogonal to this one, i.e., the *transverse velocity* is denoted with v_t (see Fig. 1).

III. Performance Bounds for Velocity Estimation

The goal of the receiver is to estimate the position $\tilde{\mathbf{p}}$ and the velocity $\mathbf{v} = [v_\mathrm{r}, v_\mathrm{t}]$ of the target, on the basis of the received signal in (1), i.e., from the $M \times N \times K$ observations along the different OFDM symbols, subcarriers and antennas. In order to concentrate on the velocity performance bounds, which is the focus of the paper, we assume the position of the target is known at the receiver, having been previously estimated together with the gain factor α of the signal path. This is possible by exploiting the information coming from the different subcarriers and/or the phase profile of the spherical impinging wave at the receiving antennas by means of near-field array processing techniques [17]. To this end, we want to analyze the performance limits on the estimation of the velocity components v_r and v_t.

The performance of a generic unbiased estimator is lower-bounded by the CRLB, which defines the lowest achievable mean-squared error in estimating the intended parameters. Starting from (1) and on the basis of the above assumptions, τ_k is known and, as a consequence, the set of unknown parameters of interest to be estimated for the CRLB analysis is $\boldsymbol{\Theta} = \{v_\mathrm{r}, v_\mathrm{t}\}$. The (i,j)-th element of the corresponding Fisher information matrix (FIM) is [18]

$$[\mathbf{J}]_{i,j} = \frac{2}{\sigma^2} \Re \left\{ \sum_{m,n,k} \left[\frac{\partial y_{m,n,k}}{\partial \boldsymbol{\Theta}_i} \right]^* \left[\frac{\partial y_{m,n,k}}{\partial \boldsymbol{\Theta}_j} \right] \right\} . \tag{3}$$

The corresponding CRLBs are obtained by inverting the FIM. Having a 2×2 matrix, it holds

$$\mathsf{CRLB}^{(v_\mathrm{r})} = \frac{1}{\det \mathbf{J}} J_{v_\mathrm{t} v_\mathrm{t}} , \qquad \mathsf{CRLB}^{(v_\mathrm{t})} = \frac{1}{\det \mathbf{J}} J_{v_\mathrm{r} v_\mathrm{r}} \tag{4}$$

where $J_{ij} = [\mathbf{J}]_{i,j}$ and $\det \mathbf{J} = J_{v_\mathrm{r} v_\mathrm{r}} J_{v_\mathrm{t} v_\mathrm{t}} - J^2_{v_\mathrm{r} v_\mathrm{t}}$.

In the following, we will revise the performance limits for velocity estimation with a single-antenna receiver (classical configuration), then extending the analysis to the case of multiple antennas.

A. Single-antenna Case

Considering a classical single input single output (SISO) bistatic configuration (i.e., $K = 1$), the Doppler shift in (2) for $k = 0$ becomes

$$\nu_0 = \frac{2}{\lambda} v \cos\gamma_0 \cos\frac{\beta_0}{2} = \frac{2}{\lambda} v_\mathrm{r} \cos\frac{\beta}{2} . \tag{5}$$

It is well-known that with a single-antenna receiver the velocity estimation is feasible along the bistatic bisector only. Thus, only the radial velocity can be estimated, and no information concerning the velocity component along the direction perpendicular to the bistatic bisector is retrieved [15]. As a consequence, we have $\mathsf{CRLB}^{(v_\mathrm{r})} = J^{-1}_{v_\mathrm{r}}$ where

$$J_{v_\mathrm{r}} = \frac{2}{\sigma^2} \Re \left\{ \sum_{m,n} \left[\frac{\partial y_{m,n,0}}{\partial v_\mathrm{r}} \right]^* \left[\frac{\partial y_{m,n,0}}{\partial v_\mathrm{r}} \right] \right\} . \tag{6}$$

leading to

$$J_{v_\mathrm{r}} = 4\, I \cos^2\frac{\beta}{2} \tag{7}$$

with

$$I = \frac{2\pi^2 MN\, \mathsf{SNR}\, (M^2-1) T^2_\mathrm{sym}}{3\lambda^2} \tag{8}$$

determining the dependence on the signal parameters, where we have defined the signal-to-noise ratio (SNR) as $\mathsf{SNR} = P\alpha^2/\sigma^2$. It can be seen from (7)-(8) that the CRLB decreases with the square of the signal duration T_obs, as $(M^2-1)T^2_\mathrm{sym} \approx T^2_\mathrm{obs}$. Moreover, an SNR gain equal to MN is obtained, thanks to the multiple observations due to the exploitation of M OFDM symbols and N subcarriers. According to (7), the estimation is not possible along the baseline, since $\beta = \pi$ (no information on v_r available). Such a condition is often called *forward scatter*; in fact, here the transmitter-to-target range variations are equal and opposite to the target-to-receiver range variations, resulting in an almost-zero Doppler shift. Differently, the accuracy is maximum where $\beta = 0$, i.e., in the so-called quasi-monostatic region. The quasi-monostatic region of a bistatic radar is the area where the bistatic geometry behaves almost like a monostatic radar—meaning that the bistatic effects (such as large bistatic angles and significant bistatic Doppler shifts) are minimal. This can happen:

- if the transmitter and the receiver are close to each other (or the target is far away), making the bistatic angle small;
- if the target is approximately on the same direction of the baseline (x-axis according to Fig. 1), i.e., its extension before the transmitter or after the receiver.

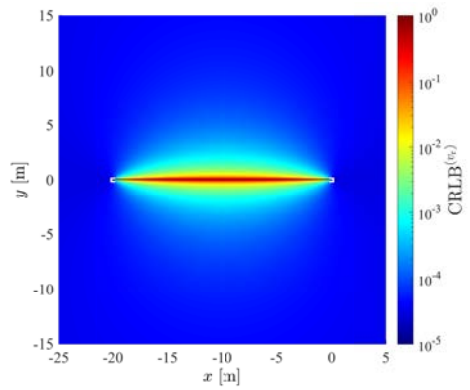

Fig. 2. CRLB for radial velocity estimation considering a SISO bistatic configuration. The white squares indicate the position of the transmitter and the receiver.

For reference, the CRLB is depicted in a 2D map in Fig. 2, where the transmitter is located in $\tilde{\mathbf{p}}_\mathrm{T} = [-20, 0]\,\mathrm{m}$ and the receiver in $\tilde{\mathbf{p}}_0 = [0, 0]\,\mathrm{m}$.[1] As expected, the estimation is infeasible along the baseline of length $L = 20\,\mathrm{m}$.

B. Multiple Antennas Case

When an antenna array and in particular an ELAA is employed, we should consider the expression in (2), as each antenna element at the receiver sees a different bistatic angle. Therefore, the antennas with indexes $k \neq 0$ experience a Doppler shift which depends also on the transverse component of the velocity v_t. For convenience, we express with $v_{\mathrm{r}k} = v\cos\gamma_k$ the k-th radial component of the velocity in (2). By introducing the angular deviation ψ_k between the target-reference antenna direction (i.e., $k = 0$) and the target-k-th antenna direction, according to Fig. 1, we have

$$\begin{aligned} v_{\mathrm{r}k} = v\cos\gamma_k &= v\cos\left(\gamma_0 - \frac{\psi_k}{2}\right) \\ &= v\cos\gamma_0\cos\frac{\psi_k}{2} + v\sin\gamma_0\sin\frac{\psi_k}{2} \\ &= v_\mathrm{r}\cos\frac{\psi_k}{2} + v_\mathrm{t}\sin\frac{\psi_k}{2} . \end{aligned} \tag{9}$$

[1]The same simulation parameters detailed in the numerical results of Sec. IV are considered.

Substituting (9) and (2) in (1), the corresponding FIM elements can be calculated as

$$J_{v_\mathrm{r}v_\mathrm{r}} = 4\,I\sum_k \cos^2\frac{\beta_k}{2}\cos^2\frac{\psi_k}{2} \tag{10}$$

$$J_{v_\mathrm{t}v_\mathrm{t}} = 4\,I\sum_k \cos^2\frac{\beta_k}{2}\sin^2\frac{\psi_k}{2} \tag{11}$$

$$J_{v_\mathrm{r}v_\mathrm{t}} = 4\,I\sum_k \cos^2\frac{\beta_k}{2}\cos\frac{\psi_k}{2}\sin\frac{\psi_k}{2} \tag{12}$$

with I defined in (8) and $\beta_k = \beta - \psi_k$ according to Fig. 1.

In order to get some simple insights into the behavior of the accuracy of estimating the radial and transverse velocity components, let us consider for simplicity a horizontal array and a target at a distance larger than the array aperture (i.e., $d > D_\mathrm{a}$). Since we have $\cos\frac{\beta_k}{2} \approx \cos\frac{\beta}{2}$ (small angles ψ_k), by exploiting the law of cosines (also known as Carnot theorem) for the triangle formed by the reference antenna - target - k-th antenna, that is $d^2 + d_k^2 - 2dd_k\cos\psi_k = x_k^2$, and trigonometric properties, (10) can be rewritten as

$$\begin{aligned} J_{v_\mathrm{r}v_\mathrm{r}} &\approx 4\,I\cos^2\frac{\beta}{2}\sum_k\cos^2\frac{\psi_k}{2} = 2\,I\cos^2\frac{\beta}{2}\sum_k(1+\cos\psi_k) \\ &= 2\,I\cos^2\frac{\beta}{2}\sum_k\left[1+\frac{1}{2}\left(\frac{d}{d_k}+\frac{d_k}{d}-\frac{x_k^2}{dd_k}\right)\right]. \end{aligned} \tag{13}$$

Considering, as first approximation, $d \approx d_k$, we obtain

$$\begin{aligned} J_{v_\mathrm{r}v_\mathrm{r}} &\approx I\cos^2\frac{\beta}{2}\sum_k\left(4-\frac{x_k^2}{d^2}\right) \\ &= KI\cos^2\frac{\beta}{2}\left[4-\frac{(K^2-1)\delta^2}{12\,d^2}\right]. \end{aligned} \tag{14}$$

Since $(K^2-1)\delta^2 \approx D_\mathrm{a}^2$ (i.e., square of the array aperture) and that we are considering a target for which $d > D_\mathrm{a}$, the right-hand term in the square bracket of (14) is much smaller than 4, so that the information on the radial velocity is practically the same of the SISO case in (7) except for a linear SNR gain K, which is expected since K independent observations are combined to estimate the Doppler shift.

For what concerns the transverse velocity estimation, by following the same procedure we have

$$\begin{aligned} J_{v_\mathrm{t}v_\mathrm{t}} &\approx 4\,I\cos^2\frac{\beta}{2}\sum_k\sin^2\frac{\psi_k}{2} = 2\,I\cos^2\frac{\beta}{2}\sum_k(1-\cos\psi_k) \\ &= 2\,I\cos^2\frac{\beta}{2}\sum_k\left[1-\frac{1}{2}\left(\frac{d}{d_k}+\frac{d_k}{d}-\frac{x_k^2}{dd_k}\right)\right] \end{aligned} \tag{15}$$

leading to

$$\begin{aligned} J_{v_\mathrm{t}v_\mathrm{t}} &\approx I\cos^2\frac{\beta}{2}\sum_k\frac{x_k^2}{d^2} = KI\cos^2\frac{\beta}{2}\frac{(K^2-1)\delta^2}{12\,d^2} \\ &\approx KI\frac{D_\mathrm{a}^2}{12\,d^2}\cos^2\frac{\beta}{2}. \end{aligned} \tag{16}$$

Thus, as evident from the approximation in (16), the fundamental figure of merit driving the capability of estimating the radial component is the aperture to distance ratio; in fact, the estimation accuracy deteriorates for large distance of the target from the receiving array, as the information scales inversally with the square of the target-receiver distance d.

IV. Numerical Results

The performance bounds on the velocity estimation are evaluated considering $f_\mathrm{c} = 28\,\mathrm{GHz}$, $M = 14$, $T_\mathrm{sym} = 66.6\,\mu\mathrm{s}$, $N = 1200$ subcarriers, and $\delta = \lambda/2$. The transmitter is placed at $\tilde{\mathbf{p}}_\mathrm{T} = [-20, 0]\,\mathrm{m}$, while the central element of the receiver is at $\tilde{\mathbf{p}}_0 = [0, 0]\,\mathrm{m}$. A constant overall SNR over the K antennas $\mathsf{SNR}_\mathrm{tot} = K\,\mathsf{SNR} = 10\,\mathrm{dB}$ is considered. Thus, the difference in performance is eventually obtained from the array geometry (e.g., aperture); of course, actual CRLB results should be scaled accordingly by a factor K. A horizontal deployment along the x axis is considered for the receiving array.

Fig. 3 reports the 2D maps of the CRLB distribution concerning the transversal velocity in a $30 \times 30\,\mathrm{m}$ area where the target is supposed to be placed. The results account for the expression (4)-right computed starting from the FIM components derived in (10)-(12) which depend on the geometry of the system (position of the transmitter, receiving array, and target) and on the signal parameters accounted by the term (8). The figure is proposed with an increasing number of antennas, i.e., $K = 11$, $K = 101$, and $K = 501$. As can be seen, when the array is small, the information on the transverse geometry is mostly unreliable in all the considered scenarios. In fact, in this case, only the radial component of the velocity can be estimated. Differently, as far as the aperture of the array becomes significant, the accuracy of the estimation for the transverse component drastically increases, especially if the target is placed in proximity of the receiving array. The accuracy of the estimation decreases when moving far away from the array (see, e.g., Fig. 3b). In fact, the possibility of collecting information on the transverse velocity derives from the capability of projecting the target velocity along the set of directions corresponding to the different antennas of the array; when the target is far away, the array is seen practically as a single point, thus estimation is not feasible. Moreover, the performance deteriorates when the target is placed in a direction close to the array deployment (e.g., in the quasi-monostatic region). Here, in fact, the direction is the same for all the antennas and corresponds to the radial direction, so no further information becomes available rather than the radial velocity. The 2D distribution of the transverse error around the array is similar to that obtained in the monostatic case in [13]; however, here the transverse velocity is calculated with respect to the bistatic bisector. It is interesting to remark that, looking at Fig. 3, the distribution is not symmetric with respect to the broadside direction of the array due to the bistatic geometry where the transmitter is placed outside the array aperture.

It is important to note that, in this case, the orientation of the receiving array can play a fundamental role. Successive work will focus on a more comprehensive analysis of the impact of the array geometry and orientation. Finally, it should be noted that, in the considered simulations, the SNR was assumed a

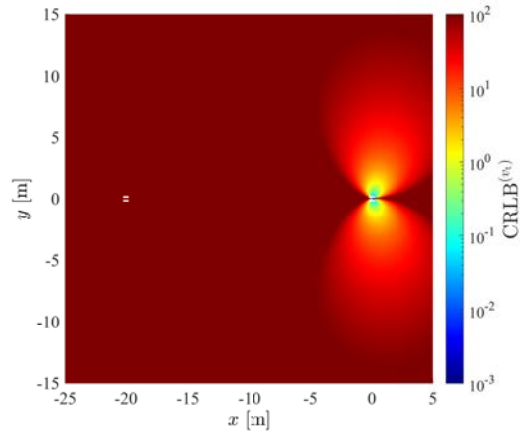

(a) $K = 11$

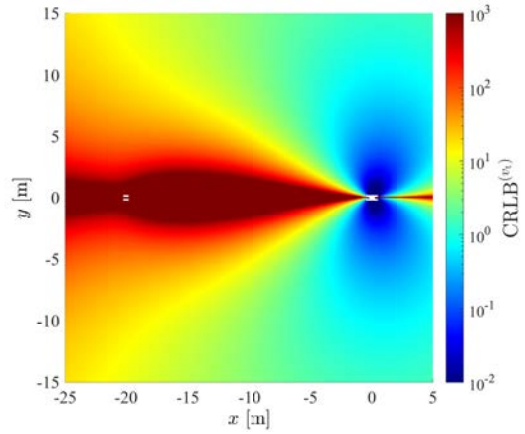

(b) $K = 101$

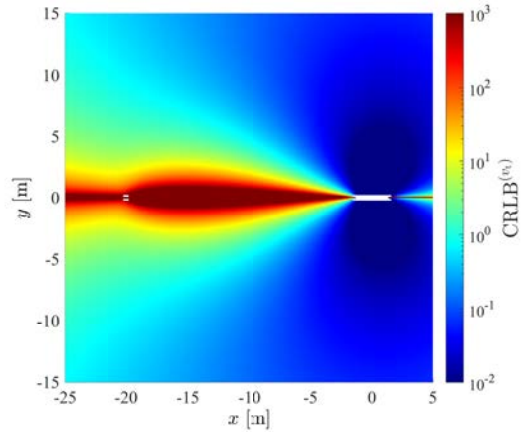

(c) $K = 501$

Fig. 3. 2D maps of the CRLB for transverse velocity estimation with antenna arrays.

constant term. In a real scenario, the target position and its radar cross section, implicitly included in α^2, may play a crucial role in the actual received power depending on the geometry, thus affecting the CRLB distribution.

V. Conclusion

This paper has demonstrated that the use of ELAAs in bistatic radar systems enables the estimation of both the radial and transverse components of the target's velocity, specifically in the proximity of the array. This represents a significant improvement over single-antenna bistatic radars, which are limited to estimating only the radial velocity component along the bistatic bisector. By deriving the CRLB, we have characterized the theoretical accuracy of velocity estimation, illustrating the impact of the array's aperture. Approximated expressions for large apertures permit to obtain simple design guidelines. Numerical simulations showed the potential of bistatic geometries, combined with large aperture arrays, to enhance target motion estimation.

References

[1] W. Tong and P. Zhu, *6G: The Next Horizon: From Connected People and Things to Connected Intelligence*. Cambridge University Press, 2021.

[2] M. F. Keskin *et al.*, "Fundamental trade-offs in monostatic ISAC: A holistic investigation towards 6G," *IEEE Trans. Wireless Commun.*, pp. 1–1, Apr. 2025.

[3] N. González-Prelcic *et al.*, "The integrated sensing and communication revolution for 6G: Vision, techniques, and applications," *Proceedings of the IEEE*, vol. 112, no. 7, pp. 676–723, July 2024.

[4] N. Decarli, A. Guerra, C. Giovannetti, F. Guidi, and B. M. Masini, "V2X sidelink localization of connected automated vehicles," *IEEE J. Select. Areas Commun.*, vol. 42, no. 1, pp. 120–133, Jan. 2024.

[5] E. Favarelli *et al.*, "Sensor fusion and resource management in MIMO-OFDM joint sensing and communication," *IEEE Trans. Veh. Technol.*, pp. 1–16, Feb. 2025.

[6] S.-G. Lee, J. Jung, and S.-C. Kim, "Enhanced velocity vector estimation using distributed radar system," in *2022 IEEE VTS Asia Pacific Wireless Communications Symposium (APWCS)*, Aug. 2022, pp. 75–79.

[7] Q. He, R. S. Blum, H. Godrich, and A. M. Haimovich, "Cramer-Rao bound for target velocity estimation in MIMO radar with widely separated antennas," in *2008 42nd Annual Conference on Information Sciences and Systems*, March 2008, pp. 123–127.

[8] M. Antoniou, H. Ma, A. Stove, and M. Cherniakov, "Target velocity estimation with multistatic GNSS-based radar," in *2018 19th International Radar Symposium (IRS)*, June 2018, pp. 1–7.

[9] M. A. Richards, *Fundamentals of radar signal processing*. McGraw-Hill, 2005.

[10] M. S. Greco, P. Stinco, F. Gini, and A. Farina, "Cramer-Rao bounds and selection of bistatic channels for multistatic radar systems," *IEEE Trans. Aerosp. Electron. Syst.*, vol. 47, no. 4, pp. 2934–2948, Oct. 2011.

[11] Z. Wang, X. Mu, and Y. Liu, "Near-field velocity sensing and predictive beamforming," *IEEE Trans. Veh. Technol.*, vol. 74, no. 1, pp. 1806–1810, Jan. 2025.

[12] H. Chen *et al.*, "6G localization and sensing in the near field: Features, opportunities, and challenges," *IEEE Wireless Commun.*, vol. 31, no. 4, pp. 260–267, Aug. 2024.

[13] C. Giovannetti, N. Decarli, and D. Dardari, "Performance bounds for velocity estimation with extremely large aperture arrays," *IEEE Wireless Communications Letters*, vol. 13, no. 12, pp. 3513–3517, Dec. 2024.

[14] C. B. Barneto *et al.*, "Full-duplex OFDM radar with LTE and 5G NR waveforms: challenges, solutions, and measurements," *IEEE Trans. Microwave Theory Tech.*, vol. 67, no. 10, pp. 4042–4054, Oct. 2019.

[15] N. J. Willis, *Bistatic Radar*, 2nd ed. The Institution of Engineering and Technology, 2004.

[16] M. F. Keskin, V. Koivunen, and H. Wymeersch, "Limited feedforward waveform design for OFDM dual-functional radar-communications," *IEEE Trans. Signal Process.*, vol. 69, pp. 2955–2970, Apr. 2021.

[17] Z. Wang, P. Ramezani, Y. Liu, and E. Björnson, "Near-field localization and sensing with large-aperture arrays: From signal modeling to processing," *IEEE Signal Processing Mag.*, vol. 42, no. 1, pp. 74–87, Jan. 2025.

[18] S. M. Kay, *Fundamentals of Statistical Signal Processing: Estimation Theory*. Upper Saddle River, NJ: Prentice-Hall, 1993.